Effect of vacancies on the heat conduction of silicon nanowires. A Molecular Dynamics Simulation Approach

Author: Marc Túnica*
Facultat de Física, Universitat de Barcelona, Diagonal 645, 08028 Barcelona, Spain.
ICMAB-CSIC, Campus de Bellaterra, 08193 Bellaterra, Spain.

Advisor: Dr. Riccardo Rurali.
Co-advisor: Prof. Miguel Rubí.

Abstract: Many experiment and theoretical results suggest a strong reduction of the thermal conductivity in silicon nanowires with respect to the bulk form. Recent experimental evidences also reported that the thermal conductivity decreases when the silicon nanowire structure is altered by the extraction of some atoms, although, few researches have focused on this topic. The aim of this report is to simulate by Molecular Dynamics the reduction of the thermal conductivity in silicon nanowires with different percentages of vacancies. The simulation method used is the Approach to Equilibrium Molecular Dynamics applying a Tersoff interaction potential. We observe that computational simulations indicates a significant variation of the heat transport due to the defect points.

Keywords: Silicon, Molecular Dynamics, Thermal conductivity, Heat transport

I. INTRODUCTION

In the field of solid states physics, several studies about the heat transport in solids have been published. Of particular concern is the thermal properties of silicon and other materials which are commonly used in electronic and thermoelectric devices. With the discovery of quantum mechanics, main resources have been destined to the research of thermoelectric properties at nanoscale. Even more, with the apparition of computer simulations, the scientific production in this field have increased exponentially. For instance, a relation between the thermal conductivity of nanowire and bulk systems was established in 1999 by Voltz and Chen [1]. Nonetheless, few investigations have focused on the effect of vacancies, a common type of intrinsic defects, in silicon nanowires. The reason can be the widely-held belief that in one-dimension systems a vacancy finds energetically convenient to segregate to the surface leading to a self-purification process, where the nanowire changes its structure by a small repositioned of the atoms around the point defect. Recent experiments [2] goes toward the opposite direction. They show that in silicon nanowires with a diameter between 170 nm and 180 nm, vacancies introduced via ion bombardment can reduce the thermal conductivity over 70%.

A common computational approach to the analysis of heat transport is the Molecular Dynamics (MD) simulation technique. It is based on the consideration of atoms as point-like particles in the space, that interact between them through a functional potential. Then, by integrating the Newton equations of motion, for each time step, the positions and velocities of each atom of our system can be calculated. Typically, the algorithms utilised to integrate the Newton equations are the Verlet algorithm or its variation, the Velocity Verlet algorithm [3]. A huge range of information can be obtained from MD simulation. We must distinguish between the coordinates and velocities of each atom and the collective properties (temperature, pressure, structure,...). For the interest of the present report, the temperature is computed by the formula

$$K_E = \frac{3}{2} N k_B T, \tag{1}$$

where k_B is the Boltzmann constant, T is the temperature, N is the number of particles and

$$K_E = \sum_{i=1}^{N} \frac{1}{2} m_i v_i^2 \tag{2}$$

is the kinetic energy, where m_i and v_i are the mass and velocity of each atom respectively [4].

Moreover, we discern between two Molecular Dynamics techniques. The Equilibrium Molecular Dynamics (EMD) is based on the Green-Kubo relation where the thermal conductivity can be estimate without considering an explicit diving force. The Non-Equilibrium Molecular Dynamics (NEMD) follows a direct method, similar to the experiments. It requires a heat flux that usually is generated by the Müller-Plathe methodology [5]. The simulation box is divided in N_s slabs perpendicular to an axis. Then, the N_s and the 0 slabs are designated as the coldest ones and the slab $N_s/2$ is the hottest. A heat flux can be achieved by exchanging the kinetic energy of the coldest atom in the hot slab with the hottest atom in the cold cell. Despite both methods are widely used, in this dissertation we follow an alternative way to compute the thermal conductivity, the Approach to equilibrium molecular Dynamics (AEMD) [6] based on the lumped capacitance [7]. It is a midpoint version be-

*Electronic address: mtunicro18@alumnes.ub.edu

tween the EMD and the NEMD, although in some references it is considered a kind of NEMD technique. In this process, we first drive the system to a controlled non-equilibrium state. Afterwards, we let the system return to the equilibrium. Each method have its advantages and disadvantages depending on the system and simulation configuration (temperature, disorder, time of simulation,....) [8].

II. OBJECTIVE

The main goal of this bachelor thesis is to study the effect of vacancies in the heat transport of silicon nanowires by the Approach to Equilibrium Molecular Dynamics (AEMD) method and a Tersoff interaction potential. We also pursue to establish a computational algorithm to achieve the disequilibrium situation necessary in the AEMD to generate a heat flux before the evolution to equilibrium.

III. METHODOLOGY

The computational method for this research is based on previous work by Melis and coworkers [10]. In the Approach to Equilibrium Molecular Dynamics, an initial non-equilibrium temperature profile can be established by dividing our simulation box in two regions with different temperatures (see figure 1a). The reader should take into account that in dielectric or intrinsic semiconductors just phonons can be considered as the main heat carriers [11]. Otherwise, in metals also electrons have a significant role.

To carry on our computing simulations, we use the library LAMMPS [12]. First of all, we construct an hexagonal silicon nanowire with a longitude of ~ 90 nm along the [111] direction and a section that can be approximated by a circle of radius $r \approx 5.00$ nm (figure 1c). It is our simulation box and it contains 87970 atoms (in the pure form) distributed initially in a perfect diamond lattice of parameter $\lambda = 5.4305$ Å. We consider non-periodical fixed bounds for the x and y directions, and along the z-axis, we impose periodical boundary conditions.

Before achieving the initial non-equilibrium state, since we are starting from all the atoms structured as a perfect diamond lattice (i.e. $T = 0$), we apply an algorithm to shake the atoms from these initial positions. We divide the process in 4 steps.

1. First, we increase the temperature from 300 K to 500 K in a canonical ensemble (NVE) simulation during 0.1 ns.

2. Afterwards, an annealing NVT process at 550 K during 0.2 ns takes place.

3. Subsequently, we cool the temperature from 500 K to 300 K with a NVE ensemble simulation during 0.22 ns.

4. Finally, we balance the structure at 300 K with a NVT process of 0.1 ns.

These previous steps are non-trivial and crucial to the correct functioning of the proceed because it provides a faultless initial disequilibrium state, far from the ideal lattice.

At this point, we divide our computational cell in two equivalent regions through the z-axis (figure 1a). Then, each region achieves different temperatures by fixing all the atoms of the other one and rescalling the velocities at each timestep [13](the ensemble of generated velocities follows a Gaussian distribution according to the temperature we assign). This action is repeated two times, one for each region, and for temperatures of 400 K and 200 K for the hot and cold division respectively. Finally, we just let the system evolve in a NVE simulation during 0.5 ns.

This algorithm is reproduced three times for each percentage of vacancies (0.00%, 0.25%, 0.50%, 0.75%, 1.00% and 1.25%). The impurities are generated uniformly along the nanowire (figure 1b) from an original x,y,z-file using a Python-Fortran script [14].

A. Thermal conductivity

The heat transport is ruled by the transport heat equation

$$\frac{\partial T}{\partial t} = \frac{\kappa}{\rho c_v}\frac{\partial^2 T}{\partial z^2}, \tag{3}$$

where ρ is the density and c_v is the specific heat. Following the previous results obtained by [10], we should consider that κ, ρ and c_v are non-time and non-z dependent variables. We also should consider periodic boundary conditions, thus, if we denote by L_z the longitude of the nanowire,

$$T(0,t) = T(L_z,t), \tag{4}$$

$$\frac{\partial T}{\partial z}(0,t) = \frac{\partial T}{\partial z}(L_z,t). \tag{5}$$

From this hypothesis, according to [10], the solution of equation (3) leads to the following expression,

$$\Delta T(t) = \sum_{n=1}^{\infty} C_n e^{-\alpha_n^2 \overline{\kappa} t}, \tag{6}$$

where $\alpha(n) = 2\pi n/L_z$, $\overline{\kappa} = \kappa/\rho c_v$ is the thermal diffusivity and

$$C_n = 8(T_{hot} - T_{cold})\frac{\left(\cos\left(\alpha_n \frac{L_z}{2}\right) - 1\right)^2}{\alpha_n^2 L_z^2}. \tag{7}$$

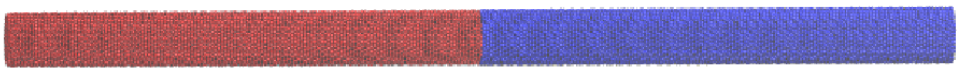

(a) Box simulation and separation between the hot and cold regions

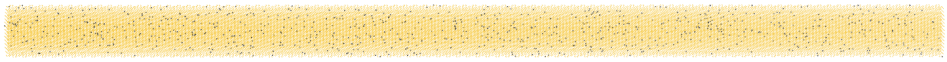

(b) Representation of the box simulation with a 1% of vacancies (black points). In this particular picture we have considered that the material is transparent, thus, we can see all the points of the nanowire.

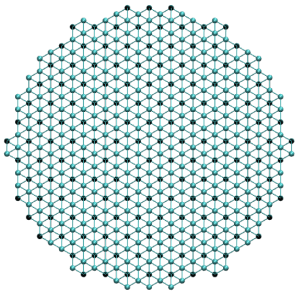

(c) Approximated hexagonal section(x-y) of the nanowire.

FIG. 1: Images obtained from the xyz coordinates file using the VMD [9] software.

Hence, to calculate the conductivity, we fit equation (6) with 26 terms to our computational results (figure 2a). For instance, figure 2b shows the fitting for a pure silicon nanowire. Afterwards, we can obtain the thermal conductivity using

$$\kappa = \overline{\kappa}\rho C_v = \frac{\overline{\kappa} C_v}{V}. \tag{8}$$

As far as we are concerned, the specific heat takes a value of $C_v = 3Nk_B$, where k_B is the Boltzmann constant. This formula was proposed for temperatures close to the Debye temperature [15]. In our case, the average temperature is 300 K, far from the Debye temperature of the silicon, around 645 K [16]. A typical solution consists to multiply the Debye heat capacity by an empirical re-escalation constant, which for an average temperature of 300 K is around $\overline{q} \approx 0.891$ [10, 17].

B. Tersoff potential

In MD, functional interatomic potentials are the most important part because they contain all the physics aspects. For our simulation, a Tersoff potential added to a Coulomb potential and a long-ranged Coulomb potential (TBC) is used. The Tersoff is a short range potential. The general form of the energy was proposed by J. Tersoff [18],

$$\begin{aligned} E &= \frac{1}{2}\sum_{i\neq j} V_{ij} \\ &= \frac{1}{2}\sum_{i\neq j} f_C(r_{ij})\left[f_R(r_{ij}+\delta) + b_{ij} f_A(r_{ij}+\delta)\right], \end{aligned} \tag{9}$$

where

$$f_R(r) = Ae^{-\lambda_1 r}, \tag{10}$$

$$f_A(r) = -Be^{-\lambda_2 r}, \tag{11}$$

$$f_C(r) = \begin{cases} 1, & if\ r < R-D, \\ 0, & if\ r > R+D, \\ \dfrac{1-\sin\left(\frac{\pi(r-R)}{2D}\right)}{2}, & otherwise, \end{cases} \tag{12}$$

with

$$b_{ij} = \left(1+\beta^n \zeta_{ij}^{n_i}\right)^{-1/(2n_i)}, \tag{13}$$

$$\zeta_{ij} = \sum_{k\neq i,j} f_C(r_{ik}+\delta) g\left(\theta_{ijk}\right) e^{\lambda_3^m (r_{ij}-r_{ik})^m}, \tag{14}$$

$$g\left(\theta\right) = \gamma\left[1 + \frac{c^2}{d^2} - \frac{c^2}{d^2 + \left(\cos(\theta) - \cos(\theta_0)\right)^2}\right]. \tag{15}$$

This particular parametrisation, tested by [19], was optimised for the study of phonon properties. The parameters of the LAMMPS' simulation [20] are summarised in table I.

IV. RESULTS AND DISCUSSION

The outcomes obtained from our computational experiments are reported in table II. Notice that the left columns correspond to the ratio of point defects and thermal conductivity of each individual simulation. The right columns comprehend its average values around 0.00%, 0.25%, 0.50%, 0.75%, 1.00% and 1.25%. Due to the lack of control in how the impurities are distributed, it can be regions with a higher density of defects. Hence, we analysed our data statistically, in groups of three simulations around the same number of particles. The error of the thermal conductivity is the sum of the standard deviation and the mean of the individual errors. The er-

Par.	**Value**	**Par.**	**Value**
γ	1	m	3
λ_3	0.0069 $\AA^{-1}$	c	99.8295
d	12.5113	$\cos\theta_0$	−0.1274
n	24.1232	β	0.6489
λ_2	1.3622 $\AA^{-1}$	B	234.6851 eV
R	3.0 $\AA$	D	0.2 $\AA$
λ_1	2.5133 $\AA^{-1}$	A	1085.7261 eV

TABLE I: Parameters of the Tersoff potential used in the AEMD simulations.

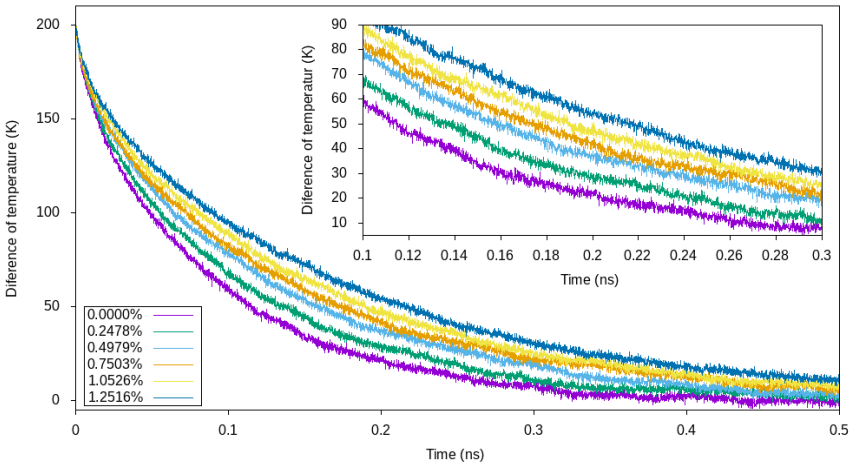

(a) Evolution of the difference of the temperature between the two regions in a NVE process for different concentration of vacancies.

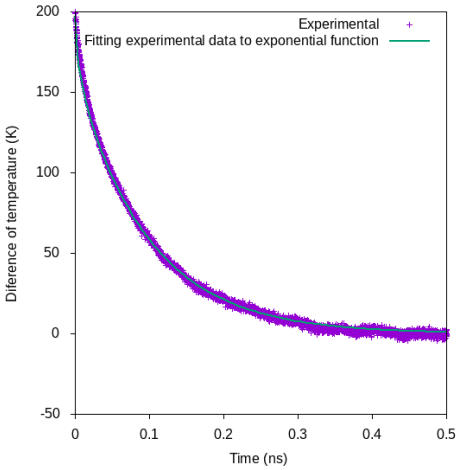

(b) Evolution of the difference of the temperature between the two regions in a NVE process for a silicon nanowire without impurities.

FIG. 2: The difference of temperature between the two regions is reduced while the system approaches to the equilibrium and each region drives to an average temperature of 300 K.

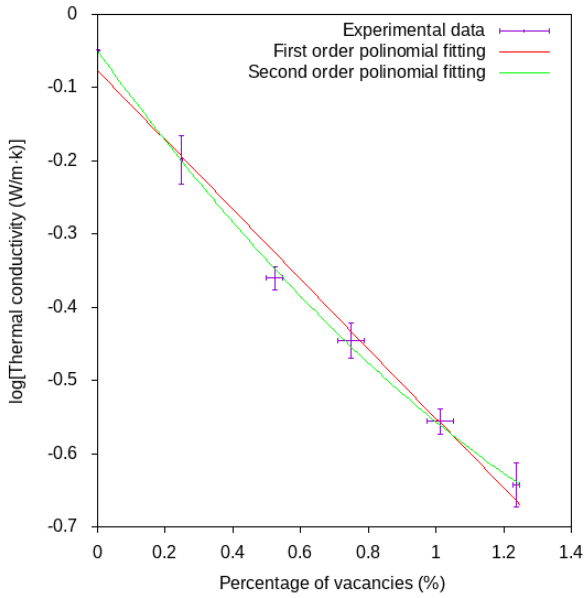

FIG. 3: Napierian logarithm of the thermal conductivity with respect to the percentage of vacancies. We add a first order and second order interpolations.

ror of the average portion of particles coincides with the standard deviation.

In figure 2a we represent the evolution of the difference between the temperatures of the hot and the cold regions. It is noteworthy that an increment of the rate of impurities leads to a detriment of the thermal conductivity and therefore a reduction of the phonon mean free path. A possible explanation to this phenomena can be a modification of the phonon group velocity and the scattering mechanisms. Moreover, in figure 3, it is showed the logarithm of the thermal conductivity as a function of the ratio of impurities. If we adjust a linear regression, we obtain a slope of $b \approx (-0.48 \pm 0.02)\%^{-1}$ and an independent term of $c \approx -0.08 \pm 0.02$, where the errors are estimated statistically from the regression (the asymptotic standard error). If we try a better adjust by adding a second term, we obtain a second order coefficient $a = (0.13 \pm 0.03)\%^{-2}$, a first order coefficient $b = (-0.64 \pm 0.03)\%^{-1}$ and an independent term $c = -0.050 \pm 0.009$.

Regarding the simulation parameters, usually, for the AEMD technique, the thermal conductivity is measured for different longitudes of the nanowire [10]. The final value is obtained from an extrapolation considering the longitude tending to infinity. Due to the limited amount of computational resources, we are not able to reproduce the process and, therefore, our thermal conductivity is underestimated. We expect the aforementioned estimation to be more in accord with the converged value if the percentage of impurities is higher because of the lessening of the mean free path of the phonons. Nonetheless, contrasting it with experimental data, it seems that at first order our approximation is within the expected values. For a 22 nm diameter, at a temperature of 300 K, it has been observed a thermal conductivity about $\kappa \leq 10$ W/(mk) [21]. Additionally, the previous paper also shows a lowering of the thermal conductivity with the reduction of the section and justify it by the effect of phonon scattering.

V. CONCLUSIONS

The methodology proposed in this investigation is useful for a low ratio of impurities and present some problems for high rates. A good improvement can be to

Individual			**Average**	
N	$\frac{N}{N_0}(\%)$	$\kappa\left(\frac{W}{Km}\right)$	$\frac{N}{N_0}(\%)$	$\kappa\left(\frac{W}{Km}\right)$
87970	0.0000	0.9526 ± 0.0008	0.0000	0.9526 ± 0.0008
87752	0.2478	0.8107 ± 0.0005	0.2489 ± 0.0009	0.8201 ± 0.0270
87750	0.2501	0.8567 ± 0.0005		
87751	0.2489	0.7934 ± 0.0005		
87532	0.4979	0.6849 ± 0.0004	0.5233 ± 0.0242	0.6974 ± 0.0112
87516	0.5161	0.7112 ± 0.0004		
87481	0.5559	0.6961 ± 0.0004		
87353	0.7014	0.6557 ± 0.0004	0.7495 ± 0.0390	0.6404 ± 0.0150
87310	0.7503	0.6208 ± 0.0004		
87269	0.7969	0.6448 ± 0.0003		
87126	0.9594	0.5651 ± 0.0003	1.0117 ± 0.0389	0.5734 ± 0.0103
87070	1.0231	0.5875 ± 0.0003		
87044	1.0526	0.5677 ± 0.0003		
86892	1.2254	0.5416 ± 0.0003	1.2375 ± 0.0108	0.5257 ± 0.0157
86883	1.2356	0.5306 ± 0.0003		
86869	1.2516	0.5048 ± 0.0002		

TABLE II: Table with the number of atoms, portion of vacancies and thermal conductivity of each simulation. The associated error corresponds to the propagation of the statistical error of the exponential fitting.

try to compute the thermal conductivity for the bulk form and add, subsequently, the surface conditions by some semiempirical method. Despite the limitations, the present research is indicative of a notorious reduction of the thermal conductivity in silicon nanowires due to the effect of vacancies. These findings provide a basis for more detailed investigations and it might be addressed in future studies, experimental and theoretical, which are also necessary to validate the kinds of conclusions that can be drawn from this report.

Acknowledgements

I would like to express my infinite gratitude to Dr. Riccardo Rurali from the Institut de Ciència de Materials de Barcelona (ICMAB-CSIC) to let me develop this bachelor thesis under his supervision. It has been a great pleasure. I also want to thank Prof. Miguel Rubí from the Department of Condensed Matter Physics from the University of Barcelona for his attention. An special gratitude to Paolo Sebastiano Floris for all his help.

[1] S.G. Volz and G. Chen. Molecular dynamics simulation of thermal conductivity of silicon nanowires. *Applied Physics Letters*, 75(14):2056, sep 1999.

[2] K. F. Murphy, B. Piccione, M. B. Zanjani, J. R. Lukes, and D. S. Gianola. Strain- and defect-mediated thermal conductivity in silicon nanowires. *Nano Letters*, 14(7):3785–3792, 2014.

[3] Loup Verlet. Computer "Experiments" on Classical Fluids. I. Thermodynamical Properties of Lennard-Jones Molecules. *Physical Review*, 159(1):98, jul 1967.

[4] compute temp command — LAMMPS documentation. `https://docs.lammps.org/compute_temp.html`.

[5] F. Müller-Plathe. A simple nonequilibrium molecular dynamics method for calculating the thermal conductivity. *The Journal of Chemical Physics*, 106(14):6082, aug 1998.

[6] E. Lampin, P. L. Palla, P. A. Francioso, and F. Cleri. Thermal conductivity from approach-to-equilibrium molecular dynamics. *Journal of Applied Physics*, 114(3):033525, jul 2013.

[7] Theodore L. Bergman, Frank P. Incropera, David P. DeWitt, and Adrienne S. Lavine. *Fundamentals of Heat and Mass Transfer*. 2002.

[8] Yuping He, Ivana Savić, Davide Donadio, and Giulia Galli. Lattice thermal conductivity of semiconducting bulk materials: atomistic simulations. *Physical Chemistry Chemical Physics*, 14(47):16209–16222, nov 2012.

[9] VMD - Visual Molecular Dynamics. `https://www.ks.uiuc.edu/Research/vmd/`.

[10] C. Melis, R. Dettori, S. Vandermeulen, and L. Colombo. Calculating thermal conductivity in a transient conduction regime: theory and implementation. *The European Physical Journal B 2014 87:4*, 87(4):1–9, apr 2014.

[11] G. P. Srivastava. The physics of phonons, 1990.

[12] LAMMPS Molecular Dynamics Simulator. `https://www.lammps.org/`.

[13] velocity command — LAMMPS documentation. `https://docs.lammps.org/velocity.html`.

[14] M. Túnica. Cretate Vacants Repository. `https://github.com/Mtunica/cretate_vacants/`.

[15] Debye Model For Specific Heat - Engineering LibreTexts. `https://eng.libretexts.org/Bookshelves/Materials_Science/Supplemental_Modules_(Materials_Science)/Electronic_Properties/Debye_Model_For_Specific_Heat`.

[16] Silicon (si), debye temperature, heat capacity, density, hardness, melting point: Datasheet from landolt-börnstein - group iii condensed matter · volume 41a1β: "group iv elements, iv-iv and iii-v compounds. part b - electronic, transport, optical and other properties".

[17] N. W. Ashcroft and N. D. Mermin. *Solid State Physics*. Holt-Saunders, 1976.

[18] Jerry Tersoff. New empirical approach for the structure and energy of covalent systems. *Physical Review B*, 37(12):6991, apr 1988.

[19] A. Rohskopf, H. R. Seyf, K. Gordiz, T. Tadano, and A. Henry. Empirical interatomic potentials optimized for phonon properties. *npj Computational Materials 2017 3:1*, 3(1):1–7, jul 2017.

[20] tersoff command — LAMMPS documentation. `https://docs.lammps.org/pair_tersoff.html`.

[21] D. Li, Y. Wu, and P. Kim. Thermal conductivity of individual silicon nanowires. *Appl. Phys. Lett*, 83:2934, 2003.